Acta Crystallographica Section F
Structural Biology and Crystallization Communications
ISSN 1744-3091

Structure of the regulatory domain of the LysR family regulator NMB2055 (MetR-like protein) from *Neisseria meningitidis*

Sarah Sainsbury,[a]*‡ Jingshan Ren,[a] Nigel J. Saunders,[b]§ David I. Stuart[a] and Raymond J. Owens[c]

[a]Division of Structural Biology, Henry Wellcome Building for Genomic Medicine, University of Oxford, Roosevelt Drive, Oxford OX3 7BN, England, [b]The Bacterial Pathogenesis and Functional Genomics Group, The Sir William Dunn School of Pathology, University of Oxford, South Parks Road, Oxford OX1 3RE, England, and [c]Oxford Protein Production Facility-UK, Research Complex at Harwell, Rutherford Appleton Laboratory, Oxfordshire OX11 0FA, England

‡ Present address: Gene Centre Munich, University of Munich – LMU, Feodor-Lynen-Strasse 25, 81377 Munich, Germany.
§ Present address: Information Systems and Computing, Heinz Wolff Building, Brunel University, Uxbridge UB8 3PH, England.

Correspondence e-mail: sainsbury@lmb.uni-muenchen.de

Received 8 December 2011
Accepted 10 March 2012

PDB References: regulatory domain of NMB2055, 4ab5; C103S/C106S mutant, 4ab6.

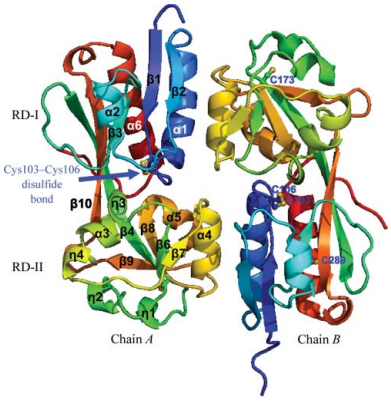

© 2012 International Union of Crystallography
All rights reserved

The crystal structure of the regulatory domain of NMB2055, a putative MetR regulator from *Neisseria meningitidis*, is reported at 2.5 Å resolution. The structure revealed that there is a disulfide bond inside the predicted effector-binding pocket of the regulatory domain. Mutation of the cysteines (Cys103 and Cys106) that form the disulfide bond to serines resulted in significant changes to the structure of the effector pocket. Taken together with the high degree of conservation of these cysteine residues within MetR-related transcription factors, it is suggested that the Cys103 and Cys106 residues play an important role in the function of MetR regulators.

1. Introduction

NMB2055 is one of six LysR-type regulators (LTTRs) encoded in the genome of the human pathogen *Neisseria meningitidis*. Exclusively found in prokaryotes, LTTRs regulate the genes of a diverse range of biological pathways, including oxidative stress and amino-acid metabolism. A typical LTTR has an approximate molecular weight of 35 kDa and comprises an N-terminal DNA-binding domain (DBD; ∼65 residues) connected *via* a linker helix (∼30 residues) to a C-terminal regulatory domain (∼200 residues). The regulatory domain (RD) adopts a fold similar to that of periplasmic binding proteins. Classically, LTTRs oligomerize to form biological tetramers which bind to DNA to repress or activate transcription in response to binding to one or more effectors (Schell, 1993). The crystal structures of several full-length LTTRs are known, including CbnR, TsaR, ArgP and AhpB (Muraoka *et al.*, 2003; Monferrer *et al.*, 2010; Zhou *et al.*, 2010; Taylor *et al.*, 2012), which form either open or closed tetramers, and two others that have distinct oligomeric states, namely CrgA, which forms an octamer (Sainsbury *et al.*, 2009), and BenM, which forms an extended array of connected dimers (Ruangprasert *et al.*, 2010).

NMB2055 shares 42% amino-acid sequence identity with MetR, a regulator of methionine biosynthesis in *Escherichia coli* and *Salmonella typhimurium*. The regulatory domains which make up most of the LysR sequence (Fig. 1*c*) share 37% sequence identity, whereas the DNA-binding domains are 47% identical. MetR was first reported as a *trans*-acting element required for the activation of *metE* and *metH*, which code for homocysteine methylases. These enzymes catalyse the final stage of methionine biosynthesis, namely the methylation of homocysteine to form L-methionine (Urbanowski *et al.*, 1987). The genes for MetE and MetR are located adjacent to each other in the genomes of both *S. typhimurium* and *E. coli* and are transcribed from divergent overlapping promoters. MetR-dependent transcription from both *metE* and *metH* is modulated by their substrate, homocysteine. Thus, in the presence of exogeneous homocysteine MetR stimulates expression of *metE* and repression of *metH* in *S. typhimurium* and *E. coli* (Urbanowski & Stauffer, 1989). Homocysteine has been shown to increase MetR DNA binding to the *S. typhimurium metE* promoter region *in vitro*, suggesting that it may interact directly with MetR, presumably through the regulatory domain of the protein (Sperandio *et al.*, 2007). Other genes regulated

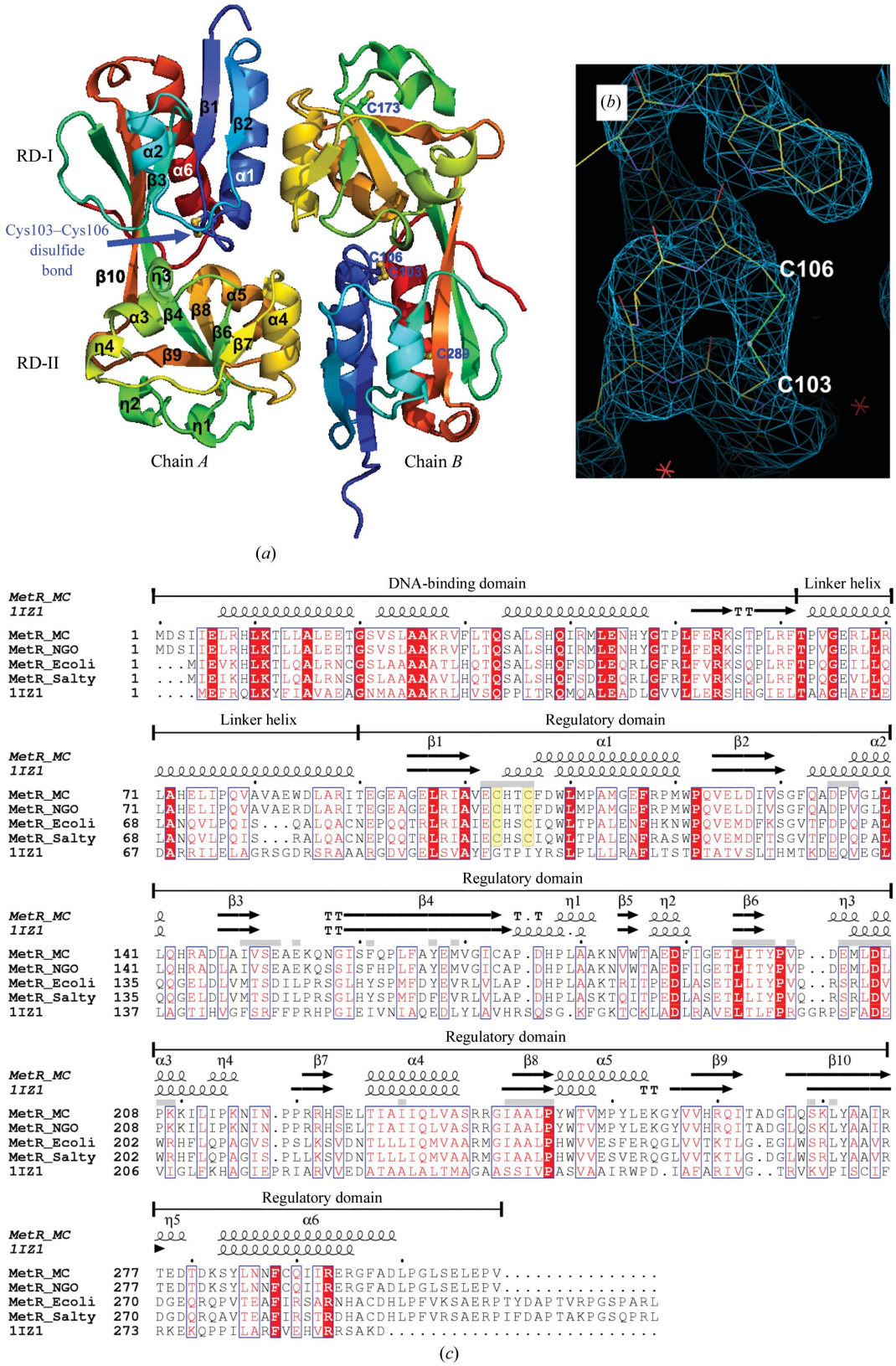

Figure 1
The structure of the NMB2055 regulatory domain shows a conserved disulfide bond in the putative effector site. (*a*) The NMB2055 regulatory-domain dimer structure solved to 2.5 Å resolution. The secondary-structure elements are labelled for chain *A* and the side chains of the cysteine residues are shown as sticks. (*b*) Unbiased initial electron density calculated by *RESOLVE* for the disulfide bond between Cys103 and Cys106 contoured at 1σ. (*c*) Multiple sequence alignment of MetR homologues and CbnR (PDB entry 1iz1; Muraoka *et al.*, 2003) with the secondary-structural elements of NMB2055 and CbnR shown. A grey line above the alignment indicates the residues that form the putative effector pocket (Dundas *et al.*, 2006). Sequence abbreviations: MC, *N. meningitidis* strain MC58; NGO, *N. gonorrhoeae* strain FA1090; Ecoli, *E. coli* strain K12; Salty, *S. typhimurium*.

in *S. typhimurium* (directly or indirectly) by MetR include *metA* (Mares *et al.*, 1992) and *glyA* (Plamann & Stauffer, 1989), which are also genes of methionine biosynthesis, and *hmp* (Poole, 2005). *Hmp* encodes flavohaemoglobin, a nitric oxide (NO) detoxifying protein (Membrillo-Hernández *et al.*, 1998; Stevanin *et al.*, 2007). In *E. coli*, MetR mediates the up-regulation of *hmp* in response to *S*-nitrosoglutathione (GSNO), which is used as an NO releaser. Since GSNO can react directly to form *S*-nitrosohomocysteine and thus deplete the cellular homocysteine pool, it is believed that the MetR-mediated regulation of *hmp* is also modulated by homocysteine. Significantly, this work established that MetR has a role in the response of bacteria to oxidative stress (Membrillo-Hernández *et al.*, 1998).

In *Neisseria* there are no evident homologues of *metA* or *hmp* and only one predicted homocysteine transmethylase (NMB0944), which shares 55% amino-acid sequence identity with MetE. However, the predicted *metE* gene is not co-located with NMB2055 in the neisserial genome. Together, these differences between *E. coli* and *S. typhimurium* on the one hand and *N. meningitidis* on the other indicate that the functions and hence the genes regulated by MetR-like proteins from different organisms may have diversified significantly.

As part of a structural genomics effort to solve the structures and understand the biological role of LTTRs in *Neisseria*, we determined the structure of the regulatory domain of the MetR-like protein NMB2055 from *N. meningitidis*. The crystal structure of the regulatory domain revealed that there is a disulfide bond between Cys103 and Cys106 located in the putative effector-binding site. The structural role of this disulfide has been investigated by generating C103S and C106S mutations and the structures of the mutant and wild-type proteins were compared.

2. Experimental methods and results

2.1. Cloning, expression and purification of NMB2055 and the regulatory domain of NMB2055

Full-length NMB2055 (Gene ID 904026) and the C-terminal regulatory domain (residues 90–309) of NMB2055 were amplified from genomic DNA (*N. meningitidis* MC58) with forward primers 5′-AAGTTCTGTTTCAGGGCCCGATGGATTCCATTATCGAATTGCGCC-3′ (FL-MetR) and 5′-AAGTTCTGTTTCAGGGCCCGACGGAAGGAGAGGCGGGAGAG-3′ (RD-MetR) and the common reverse primer 5′-ATGGTCTAGAAAGCTTTATCAGACCGGTTCCAGTTCGCTC-3′. PCR products were cloned into the vector pOPINB (Berrow *et al.*, 2007) using In-Fusion (Clontech). The constructs, which contained a 3C protease-cleavable N-terminal hexahistidine purification tag (MGSSHHHHHHSSG**LEVLFQ↓GP**; the cleavage site is shown in bold), were tested for soluble expression by semi-automated small-scale screening (Berrow *et al.*, 2007). Double cysteine-to-serine mutants (C103S/C106S) of both full-length and the regulatory domain of NMB2055 were made using PCR amplification of the vectors with primers that incorporate the desired mutations followed by treatment with *Dpn*I.

Selenomethionine-labelled and unlabelled proteins were produced in *E. coli* strain B834 (DE3) using methods described previously (Nichols *et al.*, 2009). Briefly, cells were grown at 310 K to an $OD_{600\ nm}$ of 0.6. The temperature was reduced to 293 K and protein expression was induced with 0.5 m*M* IPTG (isopropyl *β*-D-1-thiogalactopyranoside). The cells were harvested by centrifugation at 20 h post-induction. The target proteins were purified from the cleared lysate by nickel IMAC (immobilized-metal affinity chromatography) followed by gel filtration using an ÄKTAxpress platform at 277 K (GE Healthcare). The His tag was removed with rhinovirus 3C protease (the vector was kindly donated by A. Geerlof, EMBL, Hamburg) before crystallization. The cleaved proteins were passed through an nickel–IMAC column to remove the His-tagged 3C protease. 100% incorporation of selenomethionine was confirmed by mass spectrometry (Sainsbury *et al.*, 2008).

2.2. Crystallization and structure determination of the regulatory domain of NMB2055

Selenomethionine-labelled protein was concentrated to 15.5 mg ml^{-1} in 20 m*M* Tris pH 7.5, 200 m*M* NaCl, 1 m*M* TCEP. Crystallization experiments were performed in nanodrops dispensed by a Cartesian Technologies Microsys MIC4000 robot. The crystals used for data collection were optimized from the original condition of 20%(*v*/*v*) polyethylene glycol 6000, 0.1 *M* Tris pH 8.0, 0.2 *M* calcium chloride (condition No. 47 of PACT premier, Molecular Dimensions) using the standard OPPF additive screen (crystal I) or three-row (crystal II) optimization procedures described by Walter *et al.* (2005). Data were collected from crystals (space group $P2_1$) on beamline BM14 at the ESRF, Grenoble, France to 2.5 Å resolution at three wavelengths for crystal I and at a single wavelength for crystal II. Crystal I was flash-cooled in perfluoropolyether PFO-X125/03 oil (Lancaster Synthesis) and crystal II in a cryosolution consisting of 25%(*v*/*v*) glycerol and 75%(*v*/*v*) reservoir solution. Initial phases for the regulatory domain were obtained in a MAD experiment using the data collected from crystal I. 11 of a possible 12 selenium sites were identified with the *SHELX* program suite (Sheldrick, 2008). *SOLVE*/*RESOLVE* (Terwilliger, 2004) were then used for refinement of the selenium positions and phase improvement. The model was built manually using *Coot* (Emsley & Cowtan, 2004) and refined with *CNS* (Jones *et al.*, 1991) using simulated annealing and positional refinement with main-chain NCS restraints followed by individual isotropic *B*-factor refinement. The partially refined model was subsequently refined against the data from crystal II, which had a lower mosaic spread (Table 1), with *BUSTER* (Blanc *et al.*, 2004). The structure has been deposited in the PDB under accession code 4ab5.

2.3. Crystallization and structure determination of the NMB2055 regulatory domain C103S/C106S mutant

Purified NMB2055 regulatory domain C103S/C106S mutant protein was concentrated to 27 mg ml^{-1} in 20 m*M* Tris pH 7.5, 200 m*M* NaCl. Crystals used for structure determination of the C103S/C106S protein grew directly from the original screening plate in 2 *M* ammonium sulfate, 2%(*v*/*v*) polyethylene glycol 400, 100 m*M* HEPES–Na pH 7.5 (condition No. 39 of Crystal Screen, Hampton Research). Diffraction data were collected on beamline ID23.2 at the ESRF. A cryosolution consisting of 25%(*v*/*v*) glycerol and 75%(*v*/*v*) reservoir solution was added directly to the drop and the crystal was flash-cooled in liquid nitrogen. The crystals belonged to space group *H*32 and the structure was determined by molecular replacement with *MOLREP* using the wild-type regulatory-domain dimer as the input model (Lebedev *et al.*, 2008). The model was refined to a resolution of 2.8 Å with *BUSTER* (Blanc *et al.*, 2004; Table 1). The structure has been deposited in the PDB under accession code 4ab6.

3. Results

3.1. Overall structure of the regulatory domain of NMB2055

N-terminally hexahistidine-tagged versions of both full-length and the regulatory domain of the *N. meningitidis* MetR-like protein NMB2055 were purified by metal-affinity chromatography and size-

Table 1
Crystallographic statistics for the wild-type and C103S/C106S-mutant NMB2055 regulatory domains.

Values in parentheses are for the highest resolution shell.

	SeMet wild type				
	Crystal I			Crystal II	C103S/C106S mutant
Data set	Peak	Remote	Inflection	Peak	Native
Data collection					
X-ray source	BM14			BM14	ID23-EH2
Detector	MAR 225 CCD			MAR 225 CCD	MAR 225 CCD
Space group	$P2_1$			$P2_1$	$H32$
Unit-cell parameters					
a (Å)	60.9			65.2	136.9
b (Å)	52.0			52.6	136.9
c (Å)	63.4			65.9	127.8
β (°)	101.2			94.1	—
Wavelength (Å)	0.9793	0.9078	0.9795	0.9790	0.8726
Resolution range (Å)	30.0–2.50 (2.59–2.50)	30.0–2.70 (2.80–2.70)	30.0–2.70 (2.80–2.70)	30.0–2.50 (2.59–2.50)	50.0–2.80 (2.90–2.80)
Unique reflections	11655 (671)	10014 (601)	9953 (652)	13879 (826)	11470 (1128)
Completeness (%)	86.4 (50.0)†	93.2 (56.9)†	90.2 (59.4)†	89.8 (53.8)†	100 (100)
Multiplicity	9.9 (7.8)	3.7 (3.0)	3.4 (2.6)	6.4 (3.6)	18.1 (17.2)
Average $I/\sigma(I)$	34.5 (6.5)	17.0 (2.6)	17.9 (2.3)	19.6 (4.1)	21.4 (3.9)
$R_{\rm merge}$‡	0.083 (0.234)	0.056 (0.223)	0.060 (0.264)	0.097 (0.214)	0.159 (0.865)
Refinement					
Resolution (Å)				30.0–2.50	43.4–2.80
No. of reflections (working/test)				13150/700	11469/574
$R_{\rm work}/R_{\rm free}$				0.186/0.238	0.210/0.254
No. of atoms					
Protein				3446	3348
Water				182	32
Other				0	5
R.m.s.d. bonds (Å)				0.009	0.008
R.m.s.d. angles (°)				1.12	1.11
$B_{\rm Wilson}$ (Å^2)				50.5	64.5
Mean B factor (Å^2)				44.4	63.6
Ramachandran plot§ (%)					
Favoured				97.0	96.9
Allowed				3.0	2.9
Disallowed				0	0.2

† Data were processed into the corner of the detector. ‡ $R_{\rm merge} = \sum_{hkl}\sum_i |I_i(hkl) - \langle I(hkl)\rangle|/\sum_{hkl}\sum_i I_i(hkl)$. § Chen *et al.* (2010).

exclusion chromatography (SEC). The full-length protein, which has a calculated molecular weight of 34.7 kDa, had an SEC retention time corresponding to a molecular mass of 140 kDa. This indicated that the protein behaves as a tetramer, which corresponds to the typical oligomeric state of LTTRs (Muraoka *et al.*, 2003; Monferrer *et al.*, 2010). The molecular mass of the regulatory domain was estimated to be 35 kDa from size-exclusion analysis, compared with a calculated molecular weight of 25 kDa. Therefore, no clear conclusion can be drawn about the oligomeric state of the protein.

Following cleavage of the His tag, crystallization experiments were set up with both the purified full-length protein and the regulatory domain (residues 90–309). Diffracting crystals were only obtained from the regulatory-domain construct and the structure was solved to a resolution of 2.5 Å by the multiple-wavelength anomalous dispersion method using selenomethionine-substituted protein.

The crystal structure of the regulatory domain of NBM2055 contains a dimer in the asymmetric unit with the two chains of the domain arranged in a head-to-tail orientation (Fig. 1), which is very similar to the quarternary structure previously reported for other regulatory domains of LTTRs (see, for example, Ezezika *et al.*, 2007; Devesse *et al.*, 2011; Sainsbury *et al.*, 2010). Each chain of the regulatory domain comprises two subdomains of similar size that each adopt a Rossmann-like fold: RD-I (residues 92–166 and 270–307) and RD-II (residues 167–269). Residues 90–91 and 308–309 of chain *A* and residue 309 of chain *B* located at the N- or C-termini were disordered. Superimposition of the two regulatory-domain monomers showed an overall r.m.s.d. of 0.22 Å for 214 C^{α} atoms. The predicted overall electrostatic surface potential indicates that the regulatory domain of NMB2055 is largely acidic, which fits with its predicted isoelectric point of 5.0.

3.2. The putative effector pocket of the NMB2055 regulatory domain contains a disulfide bond

The regulatory-domain fold, in particular that of the first subdomain, is well conserved in LTTRs despite the low sequence identity of the regulatory domains. However, an unexpected feature of the RD-I subdomain of NMB2055 was the presence of a disulfide bridge between Cys103 and Cys106 which covalently links the end of the first β-strand (β1) to the start of α1 (Figs. 1*a* and 1*b*). The disulfide bridge is located towards the base of a pocket at the interface of the RD-I and RD-II subdomains which in other LTTRs is the binding site for small-molecule effectors (Devesse *et al.*, 2011; Ezezika *et al.*, 2007; Monferrer *et al.*, 2010). The pocket in the neisserial structure has a relatively large internal volume, with an average solvent-accessible surface volume of 1043 Å^3, but a narrow entrance of ∼8 × 6 Å (Dundas *et al.*, 2006). The area directly bordering the entrance to the pocket is highly negatively charged. Cys103 is exposed to the solvent with a solvent-accessible surface area of 42 Å^2, whereas Cys106 is almost completely buried with a solvent-accessible surface area of 1 Å^2 (Krissinel & Henrick, 2007). The CH*X*C sequence (residues 103–106) and the proximal Trp109 in NMB2055 are highly conserved, occurring in all 100 MetR homologues selected from the UniProt database for conservation analysis (32–99% sequence identity using *ClustalW*; Landau *et al.*, 2005). This suggests that the motif is functionally and/or structurally significant. 21 of the 35 residues that form

the putative effector pocket in the neisserial MetR homologue are conserved in *E. coli* MetR, with many of the 14 amino-acid substitutions being conservative changes (Fig. 1*c*). Most variations are observed in residues 203–208 (η3–α3), which form part of the base of the effector pocket, with a notable difference observed at residues Glu203 and Met204 (Set197 and Arg198 in *E. coli* MetR), which are located at the entrance to the pocket (Fig. 3*a*). The effector pocket of NMB2055 has a mixed character; it is lined with the side chains of several polar residues and a smaller number of nonpolar residues, namely Glu102, Cys103, Cys106, His104, Thr105, Ser151, Tyr167, Tyr198, Val200, Met204 and Leu205 (Fig. 3*a*, right panel).

The effector-binding pocket in the NMB2055 regulatory domain was compared with the structure of the regulatory domain of BenM bound to its inducer *cis*,*cis*-muconate. BenM regulates benzoate metabolism in *Acinetobacter baylyi* and activates a cluster of four Ben enzymes in response to the inducer (Ezezika *et al.*, 2007). Of the LTTR regulatory-domain structures available, BenM shows the highest structural similarity to the NMB2055 protein using secondary-structure matching (*SSM*; Krissinel, 2007). Comparison of the surface representations of the BenM and NMB2055 proteins shows a marked difference in the architecture of the effector-binding sites, with BenM presenting an open cleft compared with the pocket with a narrow entrance in the regulatory domain of NMB2055 (Fig. 2). However, overlays of the muconate-bound BenM structure and the regulatory-domain structure of NMB2055 shows that a comparably sized effector could be accommodated in the NMB2055 pocket (Fig. 3*a*). A second effector-binding site was identified in BenM, containing a benzoate molecule. A similar secondary effector-binding site has also been observed in the structure of the regulatory domain of DntR in complex with salicylate (Devesse *et al.*, 2011). Overlays show that the corresponding position in NMB2055 is occluded by the side chains of Trp109 and Phe165 (Fig. 3*b*).

3.3. Effects of C103S/C106S mutation on the structure of the regulatory domain of NMB2055

To investigate the structural role of the conserved cysteines in the putative effector pocket of NBM2055, single (C103S) and double (C103S/C106S) point mutants were generated. No soluble protein was obtained for the C103S mutant, presumably owing to the presence of a free thiol at Cys106, whereas the C103S/C106S mutant was purified and crystallized successfully. The C103S/C106S mutant crystals diffracted to 2.8 Å resolution and belonged to a different space group (*H*32) to the wild-type protein. A continuous model of the mutant structure could be built, with the exception of disordered residues that form part of the β2–α2 loop (chain *A*, residue 131; chain *B*, residues 131–134) and residues located at the N- or C-termini (chain *A*, residues 90–93 and 309; chain *B*, residues 90–94 and 308–309).

The regulatory domains of C103S/C106S-mutant and wild-type NMB2055 superimposed with an overall r.m.s.d. (all C^{α} atoms) of 0.8 Å, indicating that there is no large movement of the RD-I and RD-II subdomains on removal of the disulfide bond between Cys103 and Cys106. However, there were significant local changes in the

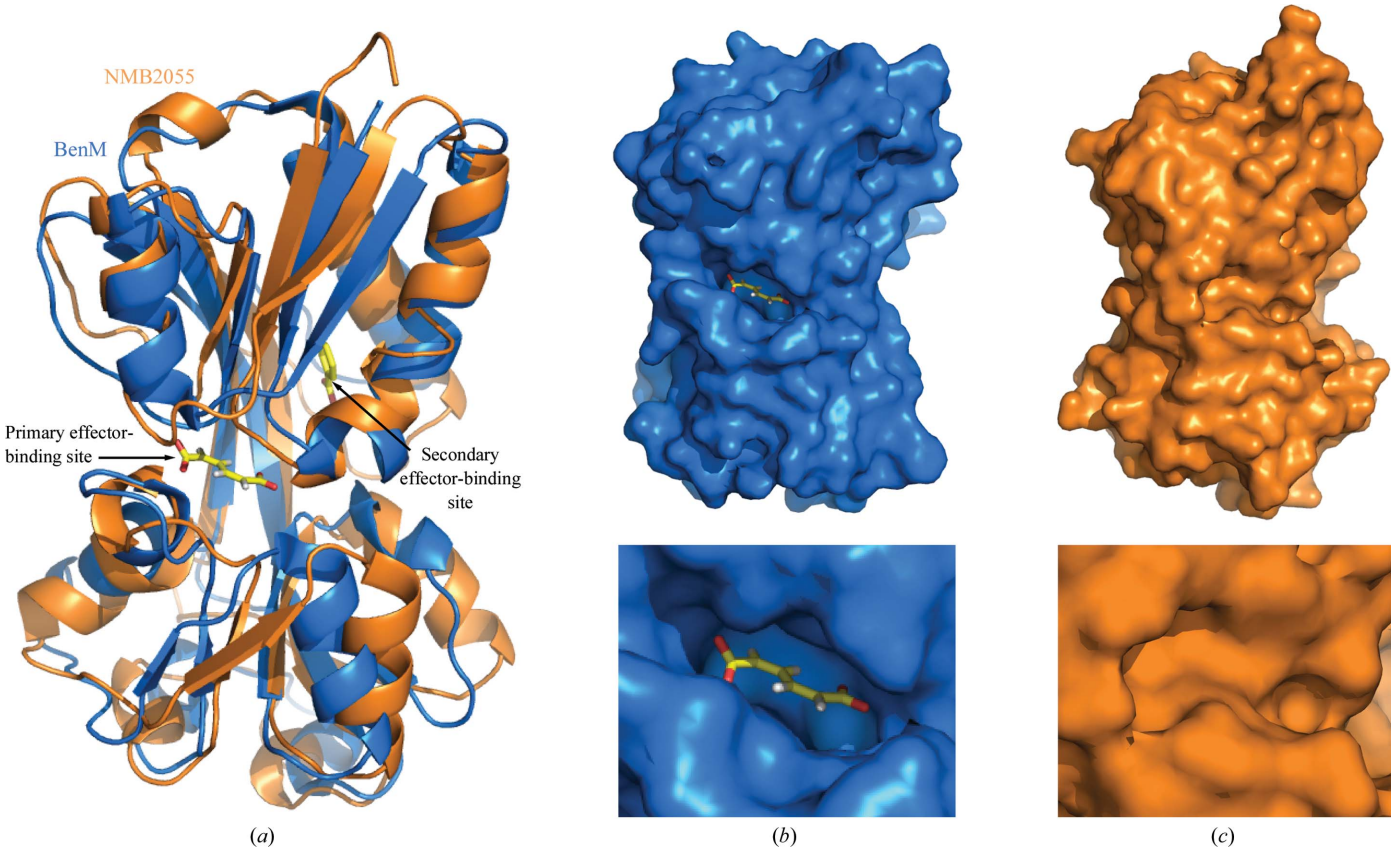

Figure 2
Comparison of the effector-bound structure of BenM (blue) with the regulatory-domain structure of NMB2055 (orange). Chain *A* of the regulatory domain of NMB2055 was superimposed onto chain *B* of BenM (PDB entry 2f7a; Ezezika *et al.*, 2007) with a core r.m.s.d. of 3.15 Å (196 residues). The effectors of BenM, *cis*,*cis*-muconate (primary binding site) and benzonate (secondary binding site), are shown as yellow sticks. (*a*) Comparison of NMB2055 and effector-bound BenM. (*b*) Surface representation of the BenM monomer and close-up of the primary effector-binding site. (*c*) Surface representation of the NMB2055 monomer and close-up of the putative primary effector-binding site.

mutant structure centred around α2 (Figs. 4*a* and 4*b*). One of the most apparent is a conformational change in the loop between the β1 and α1 elements that causes the side chain of Glu102 to point in opposite directions in the two structures, extending towards the β3–β4 loop in the C103S/C106S mutant and towards a different loop (β2–α2) in the wild-type structure. In the wild-type structure of the

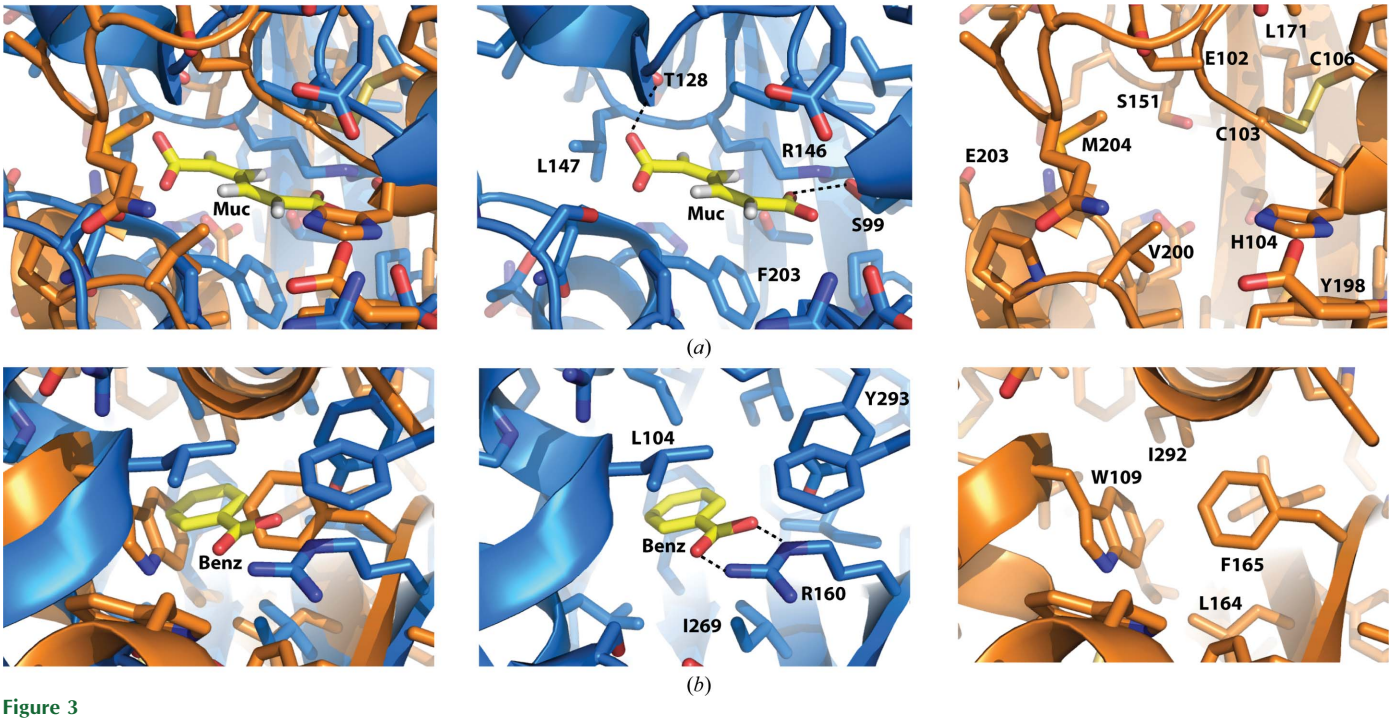

Figure 3
Comparison of the primary and secondary effector-binding sites of BenM (blue) and NMB2055 (orange). Superimposition of NMB2055 and BenM (PDB entry 2f7a) as in Fig. 2. The effectors of BenM, *cis*,*cis*-muconate (muc) and benzonate (benz), are shown as yellow sticks. (*a*) Primary effector-binding site. (*b*) Secondary effector-binding site.

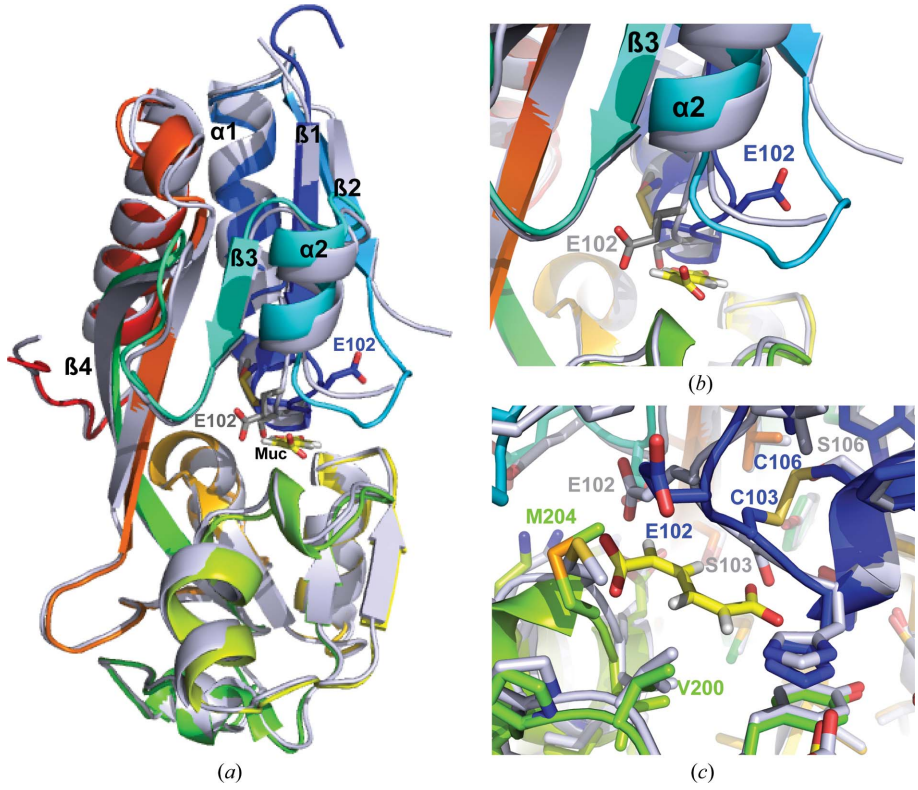

Figure 4
Effects of mutation of the Cys103 and Cys106 residues on the structure of the regulatory domain of NMB2055. Superimposition of the structures of the wild-type (coloured blue through to red) and C103S/C106S double-mutant (grey) regulatory domain of NMB2055. (*a*) Comparison of wild-type and C103/C106-mutant structures. (*b*, *c*) Close-up views of the primary effector pocket.

regulatory domain the terminal O atoms of the Glu102 side chain ($O^{\varepsilon1}$ and $O^{\varepsilon2}$) are within hydrogen-bonding distance of the three backbone N atoms of the Gly131, Phe132 and Gln133 residues of the $\beta2$–$\alpha2$ loop. As the corresponding polypeptide is disordered in the mutant structure one could reason that Glu102 has a role in stabilizing the structure of the $\beta2$–$\alpha2$ loop in the wild-type protein. In the C103S/C106S mutant Glu102 forms hydrogen bonds to the side chain and backbone N atom of Ser151, which is part of the $\beta3$–$\beta4$ loop and partially blocks the entrance to the putative effector pocket (Fig. 4). The mutated Ser103 points towards the effector pocket, while the position of Ser106 closely resembles the conformation of Cys106 in the wild-type protein (Fig. 4*c*). Associated with the above changes, there appears to be a reduction in the overall size of the effector pocket in the mutant, with an average solvent-accessible surface volume of 516 Å^3 (compared with 1043 Å^3 for the wild type; Dundas *et al.*, 2006), although one limitation of this analysis is that it does not include the disordered regions. The conformation of the residues of the RD-II subdomain which form the base of the effector pocket remains largely unchanged by the mutation (Fig. 4).

4. Discussion

On the basis of sequence homology, NMB2055 has been annotated as a methionine regulator (MetR) and is representative of a large homologous group of LysR-type transcription regulators (LTTRs). The regulatory-domain structure of *N. meningitidis* reported here is the first for this group of LTTRs. Generally, LTTRs respond to an environmental cue through the binding of a small molecule to their effector-binding pocket, which is located central to the two subdomains of the C-terminal regulatory domain (Ezezika *et al.*, 2007). Interactions between LTTRs and their co-activators appear to cause a change in the relative positions of the N-terminal DNA-binding domains, which in turn affects DNA binding and hence transcriptional activity (Taylor *et al.*, 2012). The NMB2055 structure clearly shows a disulfide bond at the base of the putative effector pocket, although it is unclear whether the formation of the disulfide bond occurred within the *E. coli* cell or through air oxidation during purification. Therefore, the oxidation state of the effector-pocket cysteines has not been established. However, given the high level of conservation of these residues amongst MetR-like LTTRs and their location in the presumed effector-binding site, it is reasonable to assume that the disulfide bridge plays a role in the function of MetR-like transcription factors. While it remains unclear what this role could be, there appears to be at least three possibilities.

(i) The disulfide bridge could provide a structural scaffold to the effector pocket. The loss of the disulfide bond in the *N. meningitidis* C103S/C106S-mutant protein clearly alters the structure around the putative binding pocket as observed in the crystal structure.

(ii) The cysteines of the disulfide bond in MetR-like proteins could play a role in redox sensing, as has been reported for a growing number of transcriptional regulators, including the LTTR OxyR (Choi *et al.*, 2001), the global regulator Spx from *Bacillus subtilis* (Nakano *et al.*, 2003), the MerR family regulator AdhR from *B. subtilis* (Nguyen *et al.*, 2009) and the Mar family regulators OhrR (Eiamphungporn *et al.*, 2009) and YodB from *B. subtilis* (Leelakriangsak *et al.*, 2008). Interestingly, Spx, which was first identified as being necessary for the growth of *B. subtilis* during oxidative stress, also contains a C*XX*C motif which upon reaction with diamide can be oxidized to a form an intramolecular disulfide bond. If the disulfide bond is accessible and reversible (*i.e.* is capable of being reduced by biologically relevant reducing agents such as reduced glutathione or homocysteine) then this would in part indicate that it could have a redox-sensing role. Whether homocysteine can bind in the effector pocket remains unresolved. There is only circumstantial evidence for direct binding of homocysteine to MetR proteins (Sperandio *et al.*, 2007) and we did not observe any electron density in cocrystallization experiments which would correspond to homocysteine in the crystal structure.

(iii) The cysteines could function to coordinate metal ions, which is often the case for proteins containing C*XX*C motifs; for example, zinc-finger proteins. Although no metal ions were detected in the structure of the NMB2055 regulatory domain and the addition of zinc to the buffer destabilized the protein to thermal denaturation (thermal shift assay; unpublished data) this possibility cannot be discounted.

The function of the MetR-like NMB2055 transcription factor in *Neisseria* remains unknown and unfortunately its genetic locus does not give any indication of what this might be since the divergent gene (*NMB2054*) is annotated as hypothetical, although it is highly conserved in *Neisseria* spp. However, the structural data reported here provide the basis for rationally investigating the functional consequences of site-specific modification of the protein.

The Oxford Protein Production Facility is funded by the Medical Research Council, with additional finance from the Biotechnology and Biological Science Research Council. We thank the beamline staff at the ESRF for help with data collection. SS was supported by an MRC studentship.

References

Berrow, N. S., Alderton, D., Sainsbury, S., Nettleship, J., Assenberg, R., Rahman, N., Stuart, D. I. & Owens, R. J. (2007). *Nucleic Acids Res.* **35**, e45.
Blanc, E., Roversi, P., Vonrhein, C., Flensburg, C., Lea, S. M. & Bricogne, G. (2004). *Acta Cryst.* D**60**, 2210–2221.
Chen, V. B., Arendall, W. B., Headd, J. J., Keedy, D. A., Immormino, R. M., Kapral, G. J., Murray, L. W., Richardson, J. S. & Richardson, D. C. (2010). *Acta Cryst.* D**66**, 12–21.
Choi, H., Kim, S., Mukhopadhyay, P., Cho, S., Woo, J., Storz, G. & Ryu, S. E. (2001). *Cell*, **105**, 103–113.
Devesse, L., Smirnova, I., Lönneborg, R., Kapp, U., Brzezinski, P., Leonard, G. A. & Dian, C. (2011). *Mol. Microbiol.* **81**, 354–367.
Dundas, J., Ouyang, Z., Tseng, J., Binkowski, A., Turpaz, Y. & Liang, J. (2006). *Nucleic Acids Res.* **34**, W116–W118.
Eiamphungporn, W., Soonsanga, S., Lee, J.-W. & Helmann, J. D. (2009). *Nucleic Acids Res.* **37**, 1174–1181.
Emsley, P. & Cowtan, K. (2004). *Acta Cryst.* D**60**, 2126–2132.
Ezezika, O. C., Haddad, S., Clark, T. J., Neidle, E. L. & Momany, C. (2007). *J. Mol. Biol.* **367**, 616–629.
Jones, T. A., Zou, J.-Y., Cowan, S. W. & Kjeldgaard, M. (1991). *Acta Cryst.* A**47**, 110–119.
Krissinel, E. (2007). *Bioinformatics*, **23**, 717–723.
Krissinel, E. & Henrick, K. (2007). *J. Mol. Biol.* **372**, 774–797.
Landau, M., Mayrose, I., Rosenberg, Y., Glaser, F., Martz, E., Pupko, T. & Ben-Tal, N. (2005). *Nucleic Acids Res.* **33**, W299–W302.
Lebedev, A. A., Vagin, A. A. & Murshudov, G. N. (2008). *Acta Cryst.* D**64**, 33–39.
Leelakriangsak, M., Huyen, N. T., Töwe, S., van Duy, N., Becher, D., Hecker, M., Antelmann, H. & Zuber, P. (2008). *Mol. Microbiol.* **67**, 1108–1124.
Mares, R., Urbanowski, M. L. & Stauffer, G. V. (1992). *J. Bacteriol.* **174**, 390–397.
Membrillo-Hernández, J., Coopamah, M. D., Channa, A., Hughes, M. N. & Poole, R. K. (1998). *Mol. Microbiol.* **29**, 1101–1112.
Monferrer, D., Tralau, T., Kertesz, M. A., Dix, I., Solà, M. & Usón, I. (2010). *Mol. Microbiol.* **75**, 1199–1214.
Muraoka, S., Okumura, R., Ogawa, N., Nonaka, T., Miyashita, K. & Senda, T. (2003). *J. Mol. Biol.* **328**, 555–566.
Nakano, S., Küster-Schöck, E., Grossman, A. D. & Zuber, P. (2003). *Proc. Natl Acad. Sci. USA*, **100**, 13603–13608.

Nguyen, T. T., Eiamphungporn, W., Mäder, U., Liebeke, M., Lalk, M., Hecker, M., Helmann, J. D. & Antelmann, H. (2009). *Mol. Microbiol.* **71**, 876–894.
Nichols, C. E., Sainsbury, S., Ren, J., Walter, T. S., Verma, A., Stammers, D. K., Saunders, N. J. & Owens, R. J. (2009). *Acta Cryst.* F**65**, 204–209.
Plamann, M. D. & Stauffer, G. V. (1989). *J. Bacteriol.* **171**, 4958–4962.
Poole, R. K. (2005). *Biochem. Soc. Trans.* **33**, 176–180.
Ruangprasert, A., Craven, S. H., Neidle, E. L. & Momany, C. (2010). *J. Mol. Biol.* **404**, 568–586.
Sainsbury, S., Lane, L. A., Ren, J., Gilbert, R. J., Saunders, N. J., Robinson, C. V., Stuart, D. I. & Owens, R. J. (2009). *Nucleic Acids Res.* **37**, 4545–4558.
Sainsbury, S., Ren, J., Nettleship, J. E., Saunders, N. J., Stuart, D. I. & Owens, R. J. (2010). *BMC Struct. Biol.* **10**, 10.
Sainsbury, S., Ren, J., Saunders, N. J., Stuart, D. I. & Owens, R. J. (2008). *Acta Cryst.* F**64**, 797–801.
Schell, M. A. (1993). *Annu. Rev. Microbiol.* **47**, 597–626.
Sheldrick, G. M. (2008). *Acta Cryst.* A**64**, 112–122.
Sperandio, B., Gautier, C., McGovern, S., Ehrlich, D. S., Renault, P., Martin-Verstraete, I. & Guédon, E. (2007). *J. Bacteriol.* **189**, 7032–7044.
Stevanin, T. M., Read, R. C. & Poole, R. K. (2007). *Gene*, **398**, 62–68.
Taylor, J. L., De Silva, R. S., Kovacikova, G., Lin, W., Taylor, R. K., Skorupski, K. & Kull, F. J. (2012). *Mol. Microbiol.* **83**, 457–470.
Terwilliger, T. (2004). *J. Synchrotron Rad.* **11**, 49–52.
Urbanowski, M. L. & Stauffer, G. V. (1989). *J. Bacteriol.* **171**, 3277–3281.
Urbanowski, M. L., Stauffer, L. T., Plamann, L. S. & Stauffer, G. V. (1987). *J. Bacteriol.* **169**, 1391–1397.
Walter, T. S. *et al.* (2005). *Acta Cryst.* D**61**, 651–657.
Zhou, X., Lou, Z., Fu, S., Yang, A., Shen, H., Li, Z., Feng, Y., Bartlam, M., Wang, H. & Rao, Z. (2010). *J. Mol. Biol.* **396**, 1012–1024.